Soil & Tillage Research 255 (2026) 106795

Contents lists available at ScienceDirect

Soil & Tillage Research

journal homepage: www.elsevier.com/locate/still

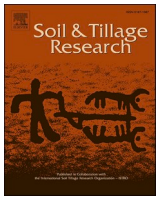

Biochar application increased soil carbon sequestration by altering organic carbon components in aggregates

Sihua Yan [a,b], Shaoliang Zhang [a,b,*], Pengke Yan [a,b], Zhimiao Wei [a,b], Xiaoguang Niu [a,b], Haijun Zhang [a,b]

[a] Northeast Agricultural University, Harbin 150030, PR China
[b] Key Substances Transportation and Regulation in Molisols, Northeast Agricultural University, Harbin 150030, PR China

ARTICLE INFO

Keywords:
Carbon-rich amendment
Water-stable aggregates
Carbon chemical component
Soil organic carbon
Mollisols

ABSTRACT

Biochar application critically influences soil organic carbon (SOC) dynamics through aggregate stabilization, but their long-term effect on the chemical components and properties of aggregate-organic carbon (OC) under crop planting remains unclear. We conducted an experiment using two biochar application methods (homogeneous application (HA), bottom-concentrated application (CA)) combined with four application amounts (0 (CK), 10 (10B), 20 (20B), 40 Mg ha^{-1}(40B)) to investigate their effect on SOC, easily-oxidized organic carbon (EOC), carbon fraction in soil aggregate, function groups of aggregate-OC and aggregate carbon preservation capacity (CPC) under maize (*Zea mays*) cropping after 6 yrs' biochar application. Results showed that compared with CK, (1) 20B and 40B increased the proportion of > 2 mm aggregates in HA while decreased it in CA but not significantly; (2) 10B increased the OC and EOC of aggregates in CA (except for 0.25–2 mm) by 13–22 % and 5–18 %, respectively, while 40B increased them in HA by 11 %-27 % and 8–28 %, respectively; (3) CA increased hydrophobicity of < 0.25 mm aggregate-OC by 2–19 %, while HA enhanced aromatic band stretching by 0.8–5 %, improving SOC resistance to microbial degradation; (4) 20B and 40B improved SOC and CPC of total water-stable aggregates but decreased EOC in HA and CA. Meanwhile, HA increased SOC by affecting aggregate-OC and its hydrophobic and aromatic functional groups, while CA increased SOC by affecting dissolved OC and aggregate-OC. Overall, a low amount of bottom-concentrated application and a higher amount of homogeneous application are promising practices to enhance the anti-microbial decomposition ability of SOC and long-term SOC sequestration.

1. Introduction

Soil organic carbon (SOC) is a key part of the soil–atmospheric carbon cycle, which is essential for mitigating climate change and maintaining soil quality (Schmitz et al., 2023). Nearly 90 % of SOC sequestration at the soil surface occurs in soil aggregates, which protect SOC through physical mechanisms limiting the accessibility of microorganisms to SOC (Kan, 2020). Because of the long-term high-intensity cultivation and unbalanced fertilization (e.g., nutrient deficiency or excessive fertilization) during farming processes, the soil structure is severely degraded, which accelerates the destruction of soil aggregates and the mineralization of organic carbon (OC) (Li et al., 2021c). Biochar, as a carbon-rich amendment material, shows potential in improving soil structural properties due to its unique porous structure and physicochemical properties, which may provide favorable conditions for SOC sequestration (Cui et al., 2020). However, it is unclear how biochar affects the soil aggregate properties and SOC sequestration after many years of application.

Soil aggregates, as an important component of soil, play an important role in the storage of soil carbon pool in farmland (Dal Ferro et al., 2023). The physical protection of OC in soil aggregates varies greatly due to the stability of different aggregate sizes (Xiao et al., 2022). Long-term biochar experiments (over several years or even decades) has generally improved aggregate stability and aggregate-OC, promoting SOC sequestration and reducing OC mineralization (Sun et al., 2022; Yang et al., 2022). This can be attributed to: (i) the oxygen functional groups on biochar surface binds to the soil organic-mineral complex, improving the stability of soil aggregates (Chen et al., 2024a); (ii) biochar promotes the transformation of silt-clay and microaggregates into large macroaggregates due to its larger specific surface area and stronger

* Corresponding author at: Northeast Agricultural University, Harbin 150030, PR China.
E-mail address: shaoliang.zhang@neau.edu.cn (S. Zhang).

https://doi.org/10.1016/j.still.2025.106795
Received 9 April 2025; Received in revised form 1 August 2025; Accepted 1 August 2025
Available online 6 August 2025

adsorption capacity, thereby enhancing the aggregation process (Deng et al., 2021; Huang et al., 2020). (iii) biochar indirectly increases root exudates and soil microorganism activity, which further promotes the formation of large macroaggregates, ultimately improving the protection and retention of OC in the soil (Yang et al., 2021). However, some short-term experiments shown that biochar has no significant or negative effect on aggregate formation, thereby reducing the protective effect of aggregate on SOC (Zhou et al., 2019). This could be due to biochar's high content of stable aromatic carbon, which is chemically stable and resistant to microbial decomposition, thereby limiting its cementation effect and delaying aggregate formation in the short term (Heikkinen et al., 2019). It can be seen that the age of biochar application is a critical attribute determining carbon sequestration capacity of soil aggregates from those hybrid processes. However, there is still limited understanding of the relationship between soil aggregate properties and SOC many years after a single biochar application, which is critical for assessing its role in SOC sequestration. Furthermore, the chemical component of SOC plays a key role in regulating its stability and microbial availability (Zhang et al., 2023). The decrease of SOC may be related to the decrease of aromatic-C and aliphatic-C in the carbon functional group, which can increase SOC mineralization and loss (Zhang et al., 2023; Tivet et al., 2013). Aliphatic C-H units characterize the SOC hydrophobicity, and its increase will decrease soil water affinity and wettability, thereby reduce the dissociation of soil aggregates and enhance SOC resistance to microbial degradation (Li et al., 2021a; Ndzelu et al., 2021; Chen et al., 2024a). Similarly, the increase of aromatic C═C units indicated a shift in SOC's chemical structure from simple to complex, enhancing its resistance to decomposition by soil microorganisms (Gao et al., 2019a, 2019b). Aliphatic-C was primarily enriched in large macroaggregates in Mollisols, while stable aromatic-C was enriched in microaggregates (Zhang et al., 2016). Thus, although physical protection and accessibility are widely recognized as key factors influencing SOC stability, the balance between soil aromatic-C and hydrophobic aliphatic-C also plays a critical role. The increase in functional groups reduces microbial accessibility and enhances aggregate stability, thereby improving SOC resistance to degradation. However, there is limited information on how biochar affects the SOC chemical components of aggregate after many years of application, which affects SOC dynamics (Deiss et al., 2021). Biochar's pyrolysis process breaks down raw materials and forms various functional groups (carboxyl, hydroxyl, carbonyl, aromatic ring and phenolic groups), contributing to nutrient absorption and carbon stabilization (Chen et al., 2024b). However, biochar application affects the chemical components and properties of aggregate-OC in soil remain unclear.

The northeast of China is one of the main distribution areas of Mollisols, known as "China's great granaries". However, long-term high-intensity tillage and erosion had caused serious soil structure degradation in Mollisols, negatively affecting agricultural productivity (Wang et al., 2022). Currently, many previous studies have focused on the effect of biochar uniformly mixed with soils on soil aggregate composition and OC (Yang et al., 2021), but this method may have adverse effects on soil animals when applied above a certain amount (Jia et al., 2023). In contrast, bottom-concentrated application of biochar (CA, biochar directly applied above the plow pan) has limited contact with the soil and may exert fewer adverse effects on soil organisms. Additionally, this method can effectively adsorb and filter nutrient ions from the solution, retain water and nutrients, and further improve crop growth (Visiy et al., 2022; Reddy et al., 2014). Previous studies have also demonstrated that CA can increase soil organic carbon and improve soil quality (Yan et al., 2022). However, the effect of CA on soil aggregate composition and OC is poorly understood, especially on the chemical components and properties of aggregate-OC after many years of biochar application. Therefore, we conducted a farmland experiment and combined with micro-Fourier transformation infrared spectroscopy (micro-FTIR) to investigate soil aggregate properties and SOC after six years of biochar application by different methods in moderately degraded Mollisols. We hypothesized that two biochar application methods can enhance the stability of SOC and promote carbon sequestration by regulating soil aggregate composition and the functional group characteristics of aggregate-OC. The aim of study is to help people deeply understand how biochar application changes the SOC sequestration by regulating the soil aggregate.

2. Materials and methods

2.1. Site and experimental materials description

The experimental area is located at the Xiangyang experimental station of Northeast Agricultural University (45°42' N, 126°36' E), in Harbin, Heilongjiang Province, China. The region is located in the monsoon zone of a temperate continental climate. The mean annual air temperature and precipitation are 3.6℃ and 500–600 mm (Li et al., 2021b). The soil type in this study area is classified as Mollisols according to the US Soil Taxonomy (Liu et al., 2011). The physicochemical properties of soil (0–20 cm) before the field trials were pH: 6.2, SOC: 17.45 g kg^{-1}, total nitrogen: 2.37 g kg^{-1}, bulk density: 0.92–0.95 g cm^{-3}, clay content (<2.00 μm): 6.8 %, silt content (2.00–20.00 μm): 65.7 % and sand content (>20.00 μm): 26.8 %. In this study, Mollisols in this farmland were classified as moderately degraded soils compared to the SOM of the 1980s (the classification of land degradation severity was detailed in Shen et al. 2006).

The biochar used in this experiment was produced by Jin Hefu Agricultural Development Co., Ltd., Liaoning, China. The biochar raw material was maize straw, which was heated at 450℃ in anaerobic conditions and the retention time of the pyrolysis process was 1 h. Biochar basic properties were pH: 9.25, total carbon: 703.8 g kg^{-1}, total nitrogen: 15.1 g kg^{-1}, total phosphorus: 7.93 g kg^{-1}, particle size: 1.5–2.0 mm; total pore volume: 0.0054 ml g^{-1}; microporous pore volume 0.0006 ml g^{-1} and average pore diameter: 16.23 mm (Yan et al., 2022).

2.2. Experimental design

Different biochar application treatments were established in the autumn of 2017 (details of the initial field establishment can be found in Yan et al. 2022). Two biochar application methods included in this study: (i) homogeneous application (HA), where the top 0–20 cm of soil was artificially removed, mixed evenly with biochar, and then refilled into the plots and gently compacted; (ii) bottom-concentrated application (CA), where the same 0–20 cm of soil was artificially removed, and biochar was evenly spread on the surface of the plow pan (at 20 cm depth) without being mixed into the soil, and then the evenly mixed original topsoil was refilled and gently compacted (Fig. S1). The control (CK) treatment adopted the same soil disturbance procedure as the biochar treatment: the top same 0–20 cm of soil was artificially removed and mixed evenly, and then refilled into the plots and gently compacted. Four biochar application amounts (0 (CK), 10 (10B), 20 (20B), and 40 (40B) Mg ha^{-1}) were included in both the HA and CA treatments. The experiment was conducted in a randomized complete block design, with each treatment having four replicated plots. Each plot had a size of 4 m^2 (2 m × 2 m). In addition, the application amounts were determined based on the application amount per unit area, and the application amounts of HA and CA were kept consistent to ensure comparability. After the experimental plot was established in October 2017, the soil remained undisturbed throughout the winter, providing natural recovery time of the soil structure's stability. Details of the experimental design can be found in Text S1 and Yan et al. (2025). Details information on fertilization and sowing in each plot from 2018 to 2023 are shown in Table S1.

2.3. Soil sample and processing

During the maize grain filling period on August 24, 2023 (after six years of biochar application), a five-point sampling method was adopted to collect undisturbed and disturbed soil samples in the 0–20 cm soil layer in each plot. For undisturbed soil samples, a spade was used to dig out vertical sections from the soil profile to maintain the original structure of the soil. The excavated soil sample was carefully packed into a hard box to ensure that the sample was not squeezed or dispersed. Avoid bumps on the way back to the lab. The plant residues (leaves, stems, roots, etc.) and rocks in the soil samples were removed. The disturbed soil samples were air-dried and then passed through a 0.154 mm sieve to determine SOC and soil easily-oxidizable organic carbon (EOC). Meanwhile, the undisturbed soil samples were lightly broken into clods with a diameter of < 1 cm along the natural structure of the soil and air-dried to determine soil water-stable aggregate size distribution, aggregate-OC, aggregate-EOC, and aggregate-OC functional groups.

2.3.1. Soil water-stable aggregates and organic carbon

The size distribution of water-stable aggregates was determined using the wet sieving method (Six et al., 1998). A 100 g aggregated soil (<1 cm) was put in the top sieve of 2, 0.25, 0.053 mm sieve stacks, and then distilled water was slowly added along the wall of the bucket until the aggregates in the top sieve were just submerged, soaking the soil sample for 10 min. The vertical stroke length of the wet sieve apparatus (LBF-100, China) is 50 mm, the oscillation time of 10 min, and the frequency of 1450 cycle/min always remained constant. Finally, soil was separated into four size classes: > 2 mm (large macroaggregates), 0.25–2 mm (small macroaggregates), 0.053–0.25 mm (microaggregates) and < 0.053 mm (silt-clay fractions). All the fractions were collected and dried at 40 °C for 12 h, weighed, ground and sieved to 0.154 mm.

The SOC content of the soil sample and aggregates was determined using a heavy cadmium acid potassium outside heating method (Kalembasa and Jenkinson, 1973) and the EOC content of the soil sample and aggregates was measured using potassium permanganate oxidation (Blair et al., 1995).

2.3.2. μ-FTIR analysis

FTIR absorbance spectra of aggregate-associated OC were recorded in the mid-infrared area of 675–4000 cm^{-1} using a micro-Fourier transformation infrared spectroscopy (μ-FTIR) (Nicolet iN10 spectrometer, Thermo Scientific, USA) in combination with ATR mode. The samples were scanned with scanning number and resolution of 16 times and 4 cm^{-1}, respectively. Air was applied for background, and the background spectrum was subtracted automatically during scanning.

To assess differences in the functional groups of aggregate-OC under different treatments, the spectra were normalized, integrated and calibrated to produce the semiquantitative results as follows. (1) Baseline correction. The software's baseline correction function was used to perform baseline correction because the spectrum obtained during the scanning process had a slight baseline inclination. (2) Calculation of the relative peak area. Determine the wavelength range of the selected absorption peak, drew a baseline within this range, integrated the absorption peaks within the range, and calculated the correction area. (3) Finally, the sum of the obtained absorption peak areas was calculated, and the percentage of each peak area was determined (i.e., the relative area of the absorption peak).

In this study, the following functional groups were selected: aliphatic C-H stretching vibration (3000–2800 cm^{-1}) (Capriel, 1997; Laudicina et al., 2015), aromatic C═C and amide C═O stretching vibrations (1650–1450 cm^{-1}) (Peltre et al., 2017), and stretching vibrations of C═O in aldehydes, ketones and carboxylic acids (1740–1710 cm^{-1}) (Ellerbrock et al., 2005). The aliphatic C-H is hydrophobic functional group, the C═O is hydrophilic functional group, and the hydrophobicity of SOC is obtained by the ratio of hydrophobic group to hydrophilic group (Simon et al., 2009; Xing et al., 2019).

2.3.3. Contribution rate of aggregate-OC and carbon preservation capacity

Contribution rate of each aggregate in total organic carbon of soil has been used to reflect the proportion of OC to total SOC in different aggregate sizes (Yang et al., 2021), carbon preservation capacity (CPC) has been described the capacity of different-sized soil aggregates to preserve carbon per unit of the specified size of water-stable aggregates (Singh and Benbi, 2018), and the equation were as below:

$$Contribution\ rate\ of\ aggregate-OC(\%) = \frac{A_i B_i}{TC_{soil}} 100\% \quad (1)$$

$$CPC(g\ \ kg^{-1} soil) = \frac{A_i B_i}{100} \quad (2)$$

$$B_i = \frac{B_{weight}}{T_{weight}} 100\% \quad (3)$$

where, A_i is SOC content of different aggregates size (g kg^{-1}); B_i is proportion of different aggregates size (%); TC_{soil} is soil total OC content (g kg^{-1}); B_{weight} is total mass of different aggregates size (g); T_{weight} is total weight of soil sample (g).

2.4. Statistical analysis

Statistical analysis and graphs were plotted with SPSS 21.0 (SPSS Inc., Chicago, USA) and Origin 2019b. Quantitative analysis in figures and tables were described as mean ± standard deviation (S.D.) of four replicates. Semi-quantitative analysis (relative peak area of characteristic peaks) in table were described as mean ± standard deviation (S.D.) of eight replicates. Quantitative and semi-quantitative data of the soil aggregate properties were screened for normal distribution using the Shapiro–Wilk test, and homogeneity of variance was determined by using Levene's test. One-way analysis of variance (ANOVA) and Tukey HSD test at the $P < 0.05$ level were used to evaluate the effects of biochar application amounts on soil properties under same application methods. And *t-test* was used to examine the difference between the different application methods under the same application amount. The single linear and nonlinear regression analyses were tested via ANOVA at $P < 0.05$. Two-Way ANOVA was used to reveal the effects of biochar application methods (A), application amount (B) and the interaction of A×B on soil aggregate properties, SOC and EOC. Spearman's correlation analysis with the "psych" and "pheatmap" package in RStudio 4.2.2 identified the relationship between carbon fraction in soil aggregate, function groups of aggregate-OC and SOC/EOC (Li et al., 2025) (http://www.r-project.org/). Partial least squares path model (PLS-PM) was used to model the relationships between the chemical component of SOC and SOC. The path coefficients and the coefficients of determination (R^2) in the path models were estimated in RStudio 4.2.2 using the "plspm" package (Sanchez, 2013) (http://www.gastonsanchez.com/PLS_Path_Modeling_with_R.pdf). The "rdacca.hp" package (Lai et al., 2022) in RStudio 4.2.2 was used to quantitatively evaluate the effects of soil aggregate properties on CPC of total water-stable aggregates.

3. Results

3.1. Soil organic carbon and easily-oxidizable organic carbon

The relationship between the SOC and biochar application amount in HA and CA could be described as a linear model and a quadratic function, respectively ($P < 0.05$) (Fig. 1a). Compared with CK, biochar application (20B and 40B) significantly increased SOC in both HA and CA ($P < 0.05$) (Fig. 1b). In contrast, biochar application decreased EOC in HA and CA, especially 10B and 20B significantly decreased EOC in HA ($P < 0.05$) (Fig. 1c). Moreover, HA had significantly higher SOC than CA under same application amount (40B) ($P < 0.05$) (Fig. 1b). SOC and

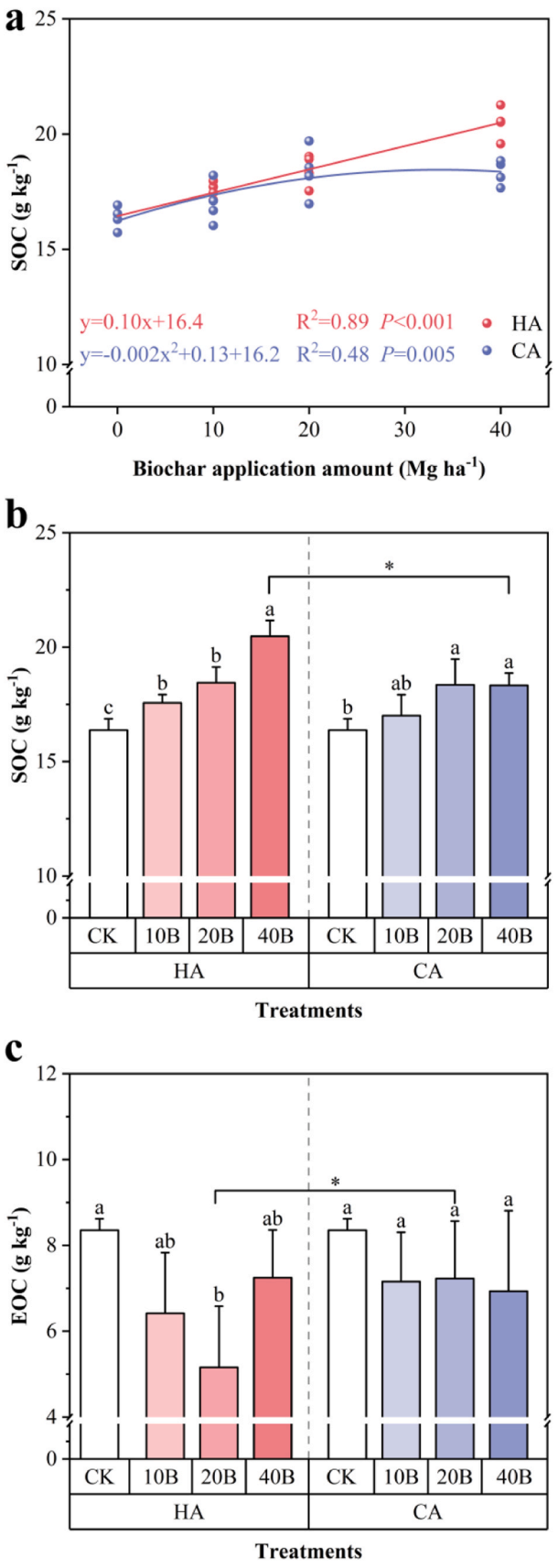

(caption on next column)

Fig. 1. Effect of biochar application methods and amounts on soil organic carbon (SOC) and easily-oxidized organic carbon (EOC). The relationship between SOC and biochar application amount (sub-figure a). Difference in content of SOC (sub-figure b) and EOC (sub-figure c) under different biochar treatments. HA, homogeneous application; CA, bottom-concentrated application; 10B, 20B and 40B, biochar application amount of 10, 20 and 40 Mg ha^{-1}, respectively in both HA and CA treatments; CK, control (no biochar). Different lowercase letters indicate differences ($P < 0.05$) in different application amounts at same application methods; brace indicate differences in different application methods at same application amounts. *$P < 0.05$.

EOC were significantly affected by A × B interactions ($P < 0.05$) (Table S3).

3.2. Soil aggregate-size distribution

The proportion of 0.25–2 mm aggregates was the highest and exceeded 40 %, while the proportions of < 0.25 mm aggregates were relatively small (Fig. 2). Compared with CK, 20B and 40B increased proportion of > 2 mm aggregates in HA, while decreased it in CA but not significantly ($P > 0.05$) (Fig. 2a). 10B significantly increased the proportions of 0.053–0.25 mm aggregates in HA ($P < 0.05$) (Fig. 2c). Meanwhile, both 10B and 40B increased the proportion of < 0.053 mm aggregates but not significantly ($P > 0.05$) (Fig. 2d). In addition, HA had significantly higher the proportion of > 2 mm aggregates and significantly lower the proportion of < 0.053 mm aggregates than CA under same application amount (20B) ($P < 0.05$) (Fig. 2a, d).

3.3. Aggregate-organic carbon and aggregate-easily-oxidizable organic carbon

Biochar application increased the OC of different diameter aggregates (Table 1). Compared with CK, 20B and 40B significantly increased > 2 mm, 0.25–2 mm and < 0.053 mm aggregate-OC in HA ($P < 0.05$). 10B significantly increased > 2 mm, 0.053–0.25 mm and < 0.053 mm aggregate-OC by 13–22 % in CA ($P < 0.05$). Moreover, HA had significantly higher > 2 mm, 0.25–2 mm and < 0.053 mm aggregate-OC than CA under same application amount (40B or 20B) ($P < 0.05$). In addition, < 0.053 mm aggregate-OC was significantly affected by A × B interactions ($P < 0.05$) (Table S2).

The effects of biochar application on the EOC of different aggregate sizes were inconsistent (Table 1). Compared with CK, 40B increased EOC in aggregate at various sizes by 8–28 % in HA, while 10B increased EOC in aggregate at various sizes (except 0.25–2 mm aggregate) by 5–18 % in CA ($P > 0.05$). 20B and 40B significantly decreased 0.25–2 mm aggregate-EOC in CA ($P < 0.05$). This indicated that HA and CA had opposite effects on the EOC in 0.25–2 mm aggregates at the highest application amount, and were significantly affected by A, B and A×B interactions ($P < 0.05$) (Table S2). Additionally, HA had significantly higher 0.053–2 mm aggregate-EOC than CA under the same application amount (40B) ($P < 0.05$).

3.4. Contribution rate of aggregate-organic carbon and carbon preservation capacity

Contribution rate of 0.25–2 mm aggregate-OC was the highest and exceeded 40 %, while contribution rate of < 0.25 mm aggregate-OC was relatively small (Fig. 3). Compared with CK, HA and CA had minimal effects on contribution rate of > 0.25 mm aggregate-OC (Fig. 3a, b). However, compared with CK, 10B significantly increased the contribution rate of 0.053–0.25 mm aggregate-OC in HA ($P < 0.05$), while 20B and 40B increased the contribution rate of 0.053–0.25 mm aggregate-OC in CA ($P > 0.05$) (Fig. 3c).

0.25–2 mm aggregate-CPC was the highest and exceeded 40 % (Fig. 4). Compared with CK, biochar application did not ($P > 0.05$) affect aggregate-CPC (except for 0.053–0.25 mm aggregates in HA)

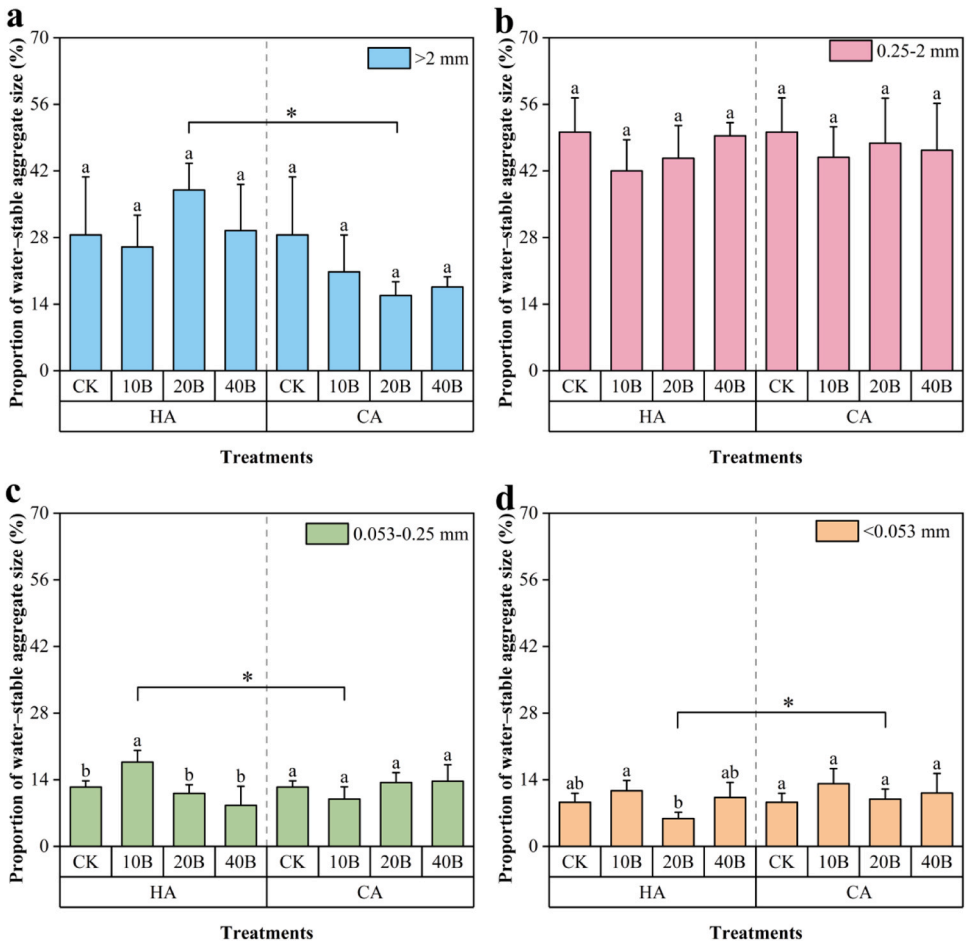

Fig. 2. Effect of biochar application methods and amounts on the proportion of > 2 mm (sub-figure a), 0.25–2 mm (sub-figure b), 0.053–0.25 mm (sub-figure c) and < 0.053 mm (sub-figure d) water-stable aggregates. HA, homogeneous application; CA, bottom-concentrated application; 10B, 20B and 40B, biochar application amounts of 10, 20 and 40 Mg ha^{-1}, respectively in both HA and CA treatments; CK, control (no biochar). Different lowercase letters indicate differences ($P < 0.05$) in different application amounts at same application methods; brace indicate differences in different application methods at same application amounts. *$P < 0.05$.

Table 1
Soil organic carbon and easily-oxidized organic carbon content in aggregates under different treatments (g kg^{-1}).

	Treatment		> 2 mm	0.25–2 mm	0.053–0.25 mm	< 0.053 mm
Soil organic carbon	HA	CK	15.63 ± 0.73c	15.58 ± 0.56b	14.51 ± 1.34a	13.27 ± 1.03b
		10B	17.72 ± 1.079bc	17.04 ± 1.82b	15.14 ± 0.97a	12.80 ± 0.43Bb
		20B	19.06 ± 1.23ab	20.12 ± 1.05Aa	16.39 ± 0.51a	15.62 ± 0.30Aa
		40B	20.62 ± 2.14Aa	19.13 ± 1.08a	16.14 ± 1.79a	16.90 ± 1.25a
	CA	CK	15.63 ± 0.73b	15.58 ± 0.56b	14.51 ± 1.34b	13.27 ± 1.03b
		10B	18.22 ± 1.30a	15.24 ± 2.08Ab	16.40 ± 0.88a	16.14 ± 1.26Aa
		20B	19.06 ± 1.23a	18.40 ± 1.18Ba	16.28 ± 0.45a	14.53 ± 0.45Bab
		40B	17.78 ± 1.21Ba	18.08 ± 0.71a	16.10 ± 0.87a	14.50 ± 2.19ab
Easily-oxidized organic carbon	HA	CK	4.60 ± 0.39a	5.15 ± 0.94ab	3.88 ± 0.26b	3.83 ± 0.22a
		10B	4.10 ± 0.55a	4.75 ± 0.84ab	4.21 ± 0.31ab	4.66 ± 1.17a
		20B	4.25 ± 0.43a	4.23 ± 0.51b	4.10 ± 0.47ab	3.74 ± 0.36a
		40B	5.18 ± 1.67a	6.19 ± 1.47Aa	4.96 ± 1.03Aa	4.12 ± 0.50a
	CA	CK	4.60 ± 0.39a	5.15 ± 0.94a	3.88 ± 0.26a	3.83 ± 0.22a
		10B	4.82 ± 0.89a	4.39 ± 0.50ab	4.59 ± 1.28a	4.41 ± 1.06a
		20B	4.43 ± 1.58a	3.74 ± 0.27b	3.92 ± 1.92a	3.00 ± 0.63a
		40B	4.52 ± 1.56a	3.79 ± 0.72Bb	3.17 ± 0.42Ba	4.44 ± 1.52a

Note: The results are presented as the means ± S.D. Different lowercase letters in a column indicate differences ($P < 0.05$) between the treatments in different application amounts at the same biochar application method, and different capital letters in a column indicate differences ($P < 0.05$) in different application methods at the same biochar application amount; there were no significant differences in the parameters with the same letter. Blue represents the key findings of the abstract, results and discussion sections. HA, homogeneous application; CA, bottom-concentrated application; 10B, 20B and 40B, biochar application amounts of 10, 20 and 40 Mg ha^{-1}, respectively in both HA and CA treatments; CK, control (no biochar).

under the same application method. Moreover, HA had significantly higher > 2 mm aggregate-CPC than CA under 20B amount, and significantly higher 0.053–0.25 mm aggregate-CPC than CA under 10B amount. It was worth mentioning that 20B and 40B significantly increased CPC of total water-stable aggregates under HA treatment compared to CK ($P < 0.05$) (Fig. 4e). Meanwhile, both application

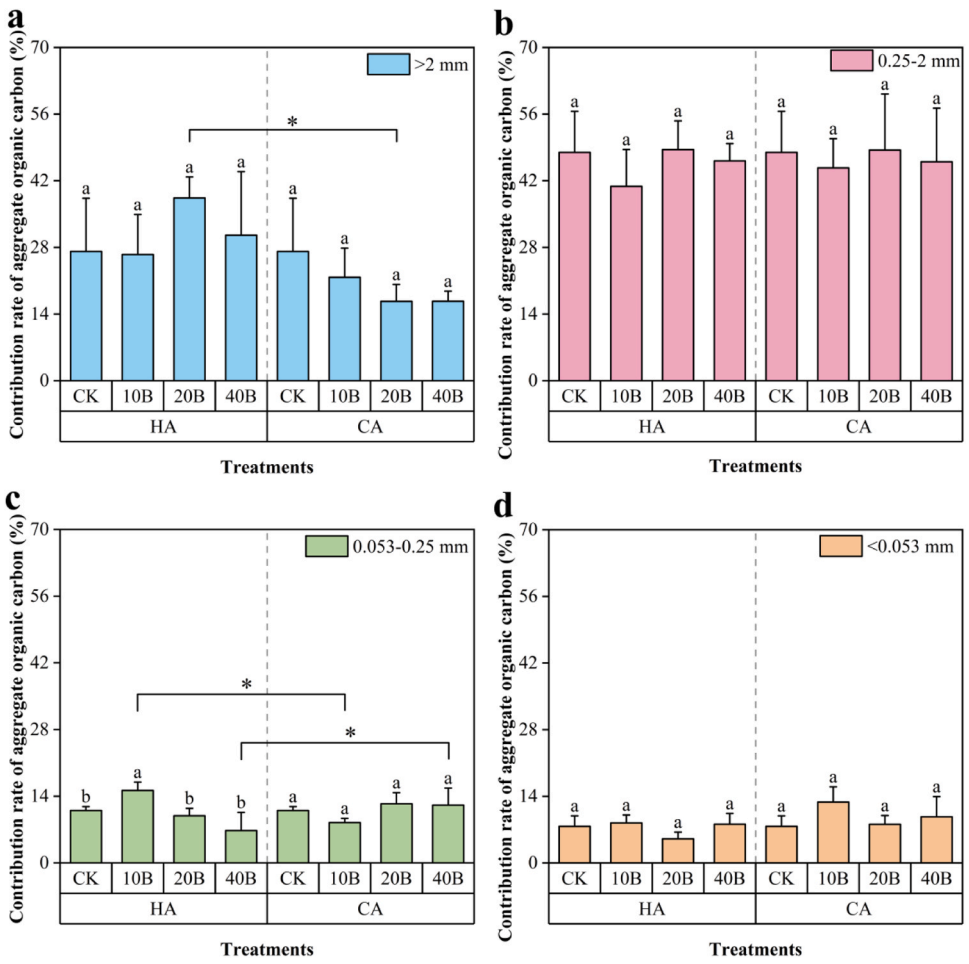

Fig. 3. Effect of biochar application methods and amounts on contribution rate of organic carbon in > 2 mm (sub-figure a), 0.25–2 mm (sub-figure b), 0.053–0.25 mm (sub-figure c) and < 0.053 mm aggregates (sub-figure d) to total organic carbon. HA, homogeneous application; CA, bottom-concentrated application; 10B, 20B and 40B, biochar application amounts of 10, 20 and 40 Mg ha^{-1}, respectively in both HA and CA treatments; CK, control (no biochar). Different lowercase letters indicate differences ($P < 0.05$) in different application amounts at same application methods; brace indicate differences in different application methods at same application amounts. *$P < 0.05$.

methods (HA and CA) exhibited linear relationships between the CPC of total water-stable aggregates and biochar application amount ($P < 0.05$) (Fig. 4f).

3.5. μ-FTIR spectra of aggregate-organic carbon

Overall, greater the hydrophilic units and smaller hydrophobic units were recorded in < 0.25 mm aggregates, and these results were opposite in > 0.25 mm aggregates (Table 2). Compared with CK, HA increased hydrophilic band stretching and decreased hydrophobicity of < 0.25 mm aggregate-OC but not significantly ($P > 0.05$). In contrast, CA all increased hydrophobicity of < 0.25 mm aggregate-OC by 2–19 % and decreased hydrophilic band stretching, with some changes were significantly different ($P < 0.05$).

Then, compared with CK, both 20B and 40B increased aromatic bands stretching of all aggregate-OC by 0.8–5 % in HA, especially significantly for < 0.053 mm aggregates ($P < 0.05$) (Table 2). This indicated that higher HA promoted the accumulation of aromatic compounds in < 0.053 mm aggregates. Meanwhile, HA had significantly higher aromatic bands stretching of < 0.25 mm aggregate-OC than CA under same application amount (40B) ($P < 0.05$) (Table 2).

3.6. Relationships among the soil aggregate, soil organic carbon and easily-oxidizable organic carbon

Spearman's rank correlation analysis showed that aggregate-OC was positively correlated with total SOC and negatively correlated with total EOC in HA and CA treatments (Fig. S2). In most cases, aggregate-OC was positively correlated with aggregate-EOC in HA, while the results were opposite in CA (Fig. s2a, b). Hydrophobicity of aggregate-OC was negatively correlated with aromatic band stretching of aggregate-OC ($P < 0.05$) (Fig. 5a, b). Additionally, there was a significant positive correlation between the aromatic band stretching of each diameter aggregate and SOC under HA ($P < 0.05$), while no such rule was found in CA (Fig. 5a, b). HA affected SOC through its effects on aromatic band stretching and hydrophobicity of aggregate-OC (Fig. 5c, e).

Additionally, the individual and common effects of soil aggregate properties on CPC of total water-stable aggregates were evaluated (Fig. 6). Besides aggregate-OC and aggregate-size distribution, which were used to calculate CPC of total water-stable aggregates, the aromatic band stretching of aggregate-OC was also an important factor (13 % and 16 %, respectively). As well, aggregate-OC and aromatic units of aggregate-OC had a high proportion of common effects on CPC of total water-stable aggregates in HA (51 %) (Fig. 6a). However, in CA, all aggregate properties had a high proportion of common effects on CPC of total water-stable aggregates (48 %) (Fig. 6b).

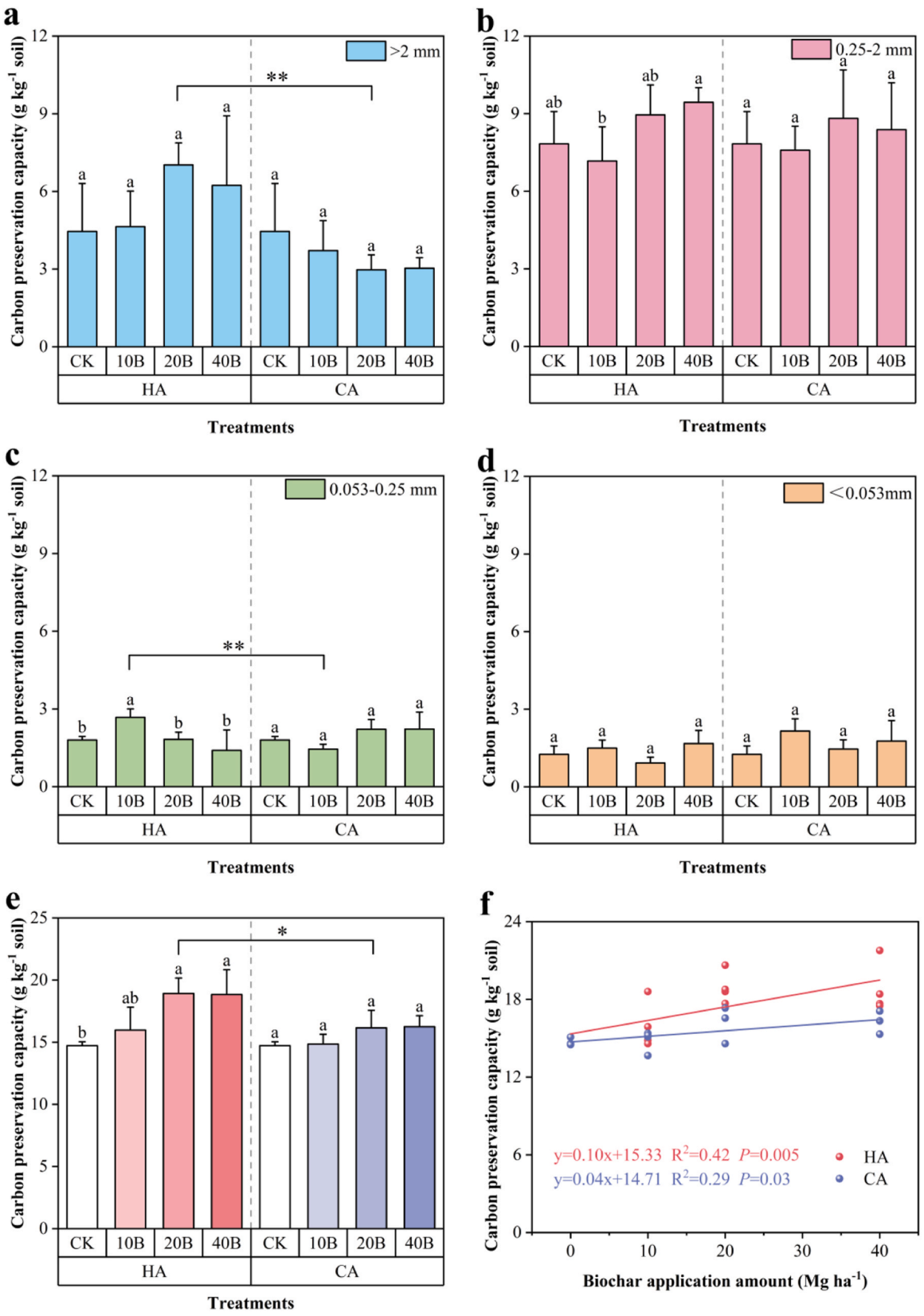

Fig. 4. Effect of biochar application methods and amounts on carbon preservation capacity in > 2 mm aggregate (sub-figure a), 0.25–2 mm aggregate (sub-figure b), 0.053–0.25 mm aggregate (sub-figure c), < 0.053 mm aggregate (sub-figure d) and total water-stable aggregates (sub-figure e). The relationship between carbon preservation capacity of total water-stable aggregates and biochar application amount (sub-figure f). HA, homogeneous application; CA, bottom-concentrated application; 10B, 20B and 40B, biochar application amounts of 10, 20 and 40 Mg ha^{-1}, respectively in both HA and CA treatments; CK, control (no biochar). Different lowercase letters indicate differences ($P < 0.05$) in different application amounts at same application methods; brace indicate differences in different application methods at same application amounts. *$P < 0.05$; **$P < 0.01$.

Table 2
Relative peak area of characteristic peaks in μ-FTIR of organic matter components in aggregates under different treatments (semi-quantitative).

Treatment		> 2 mm	0.25–2 mm	0.053–0.25 mm	< 0.053 mm
		Hydrophilic bands stretching			
HA	CK	1.68 ± 0.07a	1.73 ± 0.09a	2.14 ± 0.13a	2.00 ± 0.09a
	10B	1.70 ± 0.10a	1.72 ± 0.14a	2.19 ± 0.22a	2.08 ± 0.11Aa
	20B	1.68 ± 0.11a	1.80 ± 0.14a	2.23 ± 0.12a	2.07 ± 0.11a
	40B	1.73 ± 0.07a	1.73 ± 0.08Ba	2.21 ± 0.17Aa	2.11 ± 0.17Aa
CA	CK	1.68 ± 0.07a	1.73 ± 0.09ab	2.14 ± 0.13a	2.00 ± 0.09a
	10B	1.72 ± 0.06a	1.68 ± 0.13b	2.05 ± 0.18ab	1.93 ± 0.14Aa
	20B	1.70 ± 0.09a	1.79 ± 0.20ab	2.13 ± 0.16a	1.93 ± 0.20a
	40B	1.71 ± 0.10a	1.85 ± 0.12Aa	1.92 ± 0.13Bb	1.95 ± 0.09Ba
		Hydrophobic bands stretching			
HA	CK	3.23 ± 0.05a	3.24 ± 0.08a	3.02 ± 0.20a	3.19 ± 0.16a
	10B	3.26 ± 0.06a	3.25 ± 0.10a	2.97 ± 0.28a	3.10 ± 0.14Ba
	20B	3.21 ± 0.06a	3.21 ± 0.10a	3.11 ± 0.16a	3.11 ± 0.14a
	40B	3.21 ± 0.05Ba	3.20 ± 0.06a	3.09 ± 0.25a	3.12 ± 0.18a
CA	CK	3.23 ± 0.05a	3.24 ± 0.08a	3.02 ± 0.20b	3.19 ± 0.16a
	10B	3.22 ± 0.04a	3.23 ± 0.09a	3.16 ± 0.16ab	3.23 ± 0.06Aa
	20B	3.26 ± 0.16a	3.24 ± 0.07a	3.11 ± 0.19ab	3.15 ± 0.11a
	40B	3.28 ± 0.06Aa	3.26 ± 0.11a	3.24 ± 0.07a	3.17 ± 0.07a
		Hydrophobicity			
HA	CK	1.92 ± 0.08a	1.88 ± 0.12a	1.42 ± 0.17a	1.60 ± 0.16a
	10B	1.92 ± 0.10a	1.90 ± 0.17a	1.38 ± 0.26a	1.50 ± 0.14Ba
	20B	1.93 ± 0.14a	1.79 ± 0.17a	1.40 ± 0.12a	1.51 ± 0.13a
	40B	1.85 ± 0.10a	1.85 ± 0.09a	1.41 ± 0.18Ba	1.49 ± 0.21a
CA	CK	1.92 ± 0.08a	1.89 ± 0.12a	1.42 ± 0.17b	1.60 ± 0.16a
	10B	1.87 ± 0.09a	1.94 ± 0.19a	1.55 ± 0.20ab	1.68 ± 0.14Aa
	20B	1.92 ± 0.15a	1.83 ± 0.23a	1.47 ± 0.17b	1.65 ± 0.17a
	40B	1.92 ± 0.13a	1.77 ± 0.15a	1.69 ± 0.15Aa	1.63 ± 0.10a
		Aromatic bands stretching			
HA	CK	12.51 ± 0.33b	12.63 ± 0.28a	13.72 ± 0.20a	12.77 ± 0.30b
	10B	12.79 ± 0.27ab	12.58 ± 0.61a	13.62 ± 0.69a	13.04 ± 0.22ab
	20B	12.82 ± 0.27ab	12.87 ± 0.30a	13.84 ± 0.57a	13.34 ± 0.39Aa
	40B	12.96 ± 0.30a	12.96 ± 0.10a	13.90 ± 0.47Aa	13.45 ± 0.54Aa
CA	CK	12.51 ± 0.33a	12.63 ± 0.28a	13.72 ± 0.20a	12.77 ± 0.30a
	10B	12.59 ± 0.29a	12.57 ± 0.38a	13.29 ± 0.51ab	12.82 ± 0.34a
	20B	12.64 ± 0.17a	12.82 ± 0.52a	13.47 ± 0.58a	12.66 ± 0.53Ba
	40B	12.72 ± 0.19a	12.77 ± 0.36a	12.92 ± 0.27Bb	12.76 ± 0.30Ba

Note: The results are presented as the means ± S.D. Different lowercase letters in a column indicate differences ($P < 0.05$) between the treatments in different application amounts at the same biochar application method, and different capital letters in a column indicate differences ($P < 0.05$) in different application methods at the same biochar application amount; there were no significant differences in the parameters with the same letter. Blue represents the key findings of the abstract, results and discussion sections. HA, homogeneous application; CA, bottom-concentrated application; 10B, 20B and 40B, biochar application amounts of 10, 20 and 40 Mg ha^{-1}, respectively in both HA and CA treatments; CK, control (no biochar).

4. Discussion

4.1. Soil aggregate distribution and aggregate carbon

Soil aggregates are a critical indicator used to assess soil health, which affects soil nutrients and water movement (Li et al., 2021a). In our study, under the same application method, biochar application increased the proportion of > 2 mm aggregates in HA while decreased it in CA compared with CK, but neither was significant (Fig. 2a). It was not an unexpected result, as the formation of soil aggregates was a function of biological activity and time. The coarse biochar particle size in our study may have limited soil-microbe-biochar interactions, which might be responsible for the insignificant effect on soil aggregation (Zhang et al., 2015). Interestingly, we also found at the same amount (20B), HA had significantly higher the proportion of > 2 mm aggregates and significantly lower < 0.053 mm aggregates than CA (Fig. 2a, d). It may be that HA directly increased SOC accumulation (Fig. 2a), thereby providing the organic colloids to soil aggregates (Xu et al., 2024). This process likely promoted the formation of < 0.053 mm aggregates into > 2 mm aggregates (Fig. 2d). Conversely, the result of CA was largely driven by its indirect impact on soil moisture distribution (Fig. S3). Specifically, the relatively concentrated biochar application and its oxygen-containing functional groups and larger specific surface area greatly affected the biochar's hygroscopic process (Zhao et al., 2017). And, soil moisture monitoring results showed that the higher amounts of biochar layer in CA absorbed more soil moisture from 0–20 cm soil layer, which indirectly decreased soil moisture in the upper soil (Fig. S3). This process may reduce adhesion between the aggregates, resulting in easier dissociation from > 2 mm aggregates to < 0.053 mm aggregates. Furthermore, biochar's indirect impact on water availability may also influence microbial activity, as microbial growth and organic matter decomposition are sensitive to soil moisture fluctuations (Francoys et al., 2024). Reduced microbial activity in drier soils could further limit aggregate stability and aggravate the fragmentation process in CA treatment. This also resulted in the proportion of < 0.053 mm aggregates of CA being higher than in HA (Fig. 2d). Therefore, CA may promote the dissociation of large macroaggregates into silt-clay fractions, while the results were opposite in HA in long-term experiments, which remain to be further elucidated.

Soil aggregates play an important role in soil carbon sequestration, and there is an interdependent relationship between soil aggregates and SOC (Zhu et al., 2021). In our study, biochar increased OC in different aggregate sizes, with greater enrichment in > 0.25 mm aggregates (Table 1). Our results were supported by Xu et al. (2024), biochar's carbonylated aromatic structure contributed to OC stabilization by resisting microbial decomposition and enhancing physical protection (Kuzyakov et al., 2014; Huang et al., 2020). Thus, the biochar application can increase OC with different aggregate sizes, and it was preferentially fixed in > 0.25 mm aggregates. In addition, 40B significantly increased < 0.053 mm aggregate-OC under HA treatment, while 10B significantly increased it under CA treatment (Table 1). This may be due to: (1) high soil pH induced by biochar may promote clay flocculation and soil aggregation, enhancing OC entrapment (Xu et al., 2024; Chen et al., 2022); (2) high pH of biochar declined enzyme activities and metabolic quotient (Chen et al., 2022). The OC in soil aggregates would be accumulated due to the minor decomposition and mineralization of OC; (3) finally, < 0.053 mm aggregate showed a high response, which may be related to their larger specific surface area and stronger adsorption capacity, enabling them to better contact with ions in the soil solution and respond faster to pH changes (Xu et al., 2024). Meanwhile, these aggregates also have a higher capacity to adsorb more organic matter and minerals. This property enabled them to more effectively stabilize OC under higher pH conditions, thereby enhancing its physical protection. Previous studies have shown that < 0.053 mm aggregates responded strongly to changes in soil pH, so they may effectively store and stabilize OC through this mechanism (Xu et al., 2021). Meanwhile, low CA increased the proportion of < 0.053 mm aggregate also contributed to this result (Fig. 2d). Thus, the accumulation of OC in < 0.053 mm aggregates may be due to the combined effect of biochar-induced changes in pH, reduced microbial decomposition, and strong adsorption capacity of fine particles.

Additionally, unlike most previous studies that mainly focused on the impact of biochar application on labile OC in the whole soil, our study focuses on the impact of biochar on labile OC in soil aggregates. In this study, we found that 40B increased 0.25–2 mm aggregate-EOC in HA,

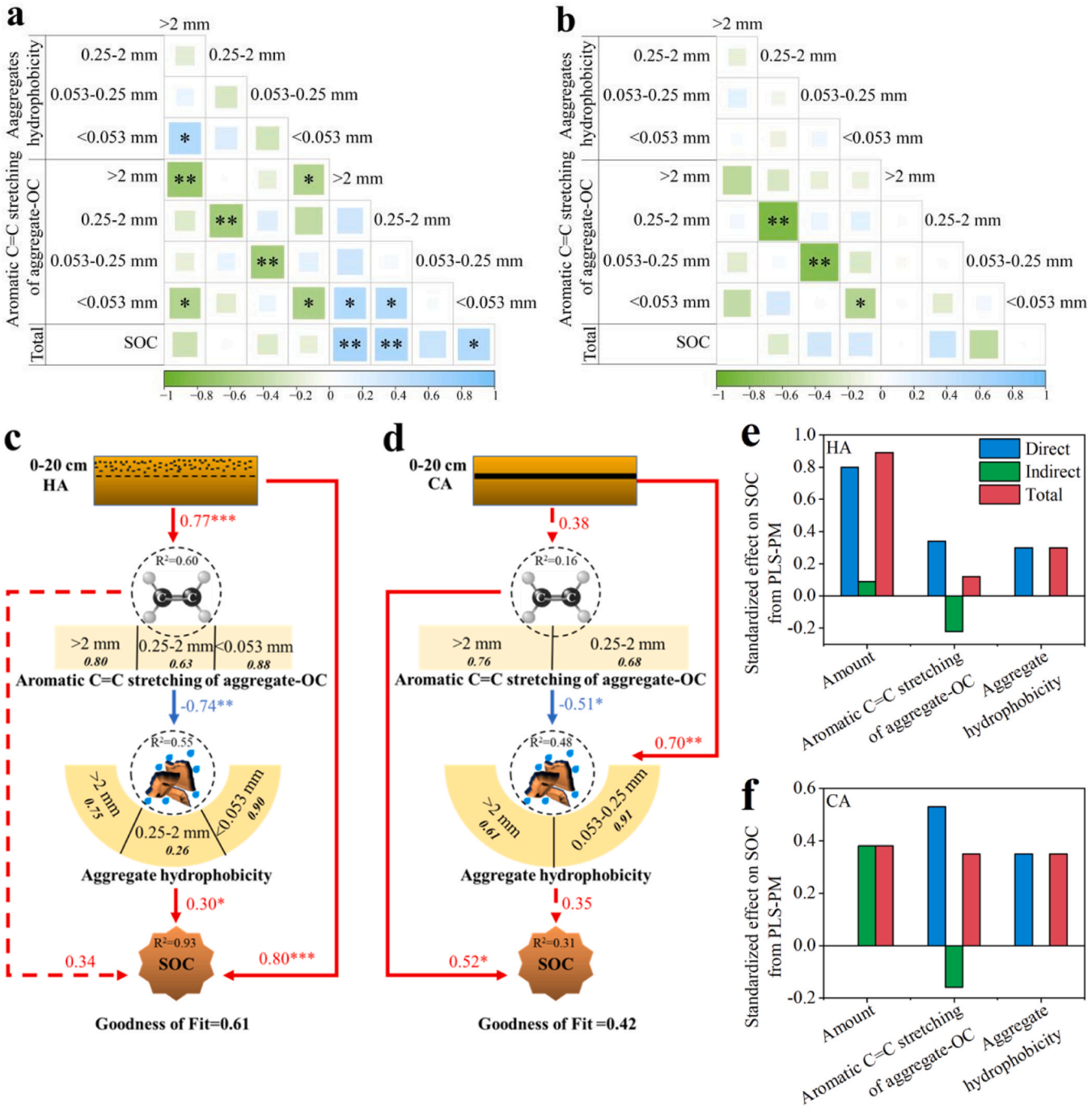

Fig. 5. Spearman's rank correlation and partial least squares modeling (PLS-PM) showing the relationships between aromatic C═C stretching of aggregate-OC, aggregate-OC hydrophobicity and soil organic carbon (SOC). Spearman's rank correlation among aromatic C═C stretching of aggregate-OC, aggregate-OC hydrophobicity and SOC under homogeneous application (HA) (sub-figure a) and bottom-concentrated application (CA) (sub-figure b). PLS-PM showing the direct and indirect effects of organic carbon chemical components within aggregates on SOC under HA (sub-Figs. c and e) and CA (sub-Figs. d and f) treatments. Red and blue lines represent positive and negative effects, respectively, and the dotted line represent non-significant relationships. $^{*}P < 0.05$, $^{**}P < 0.01$, $^{***}P < 0.001$. R^2 values indicate the variance of variables explained by the factor. Italics numbers represent the loadings of variables.

while it was opposite in CA (Table 1). This is due to high amounts of biochar application in HA provided a large number of adsorption sites, which enhanced the physical and chemical protection of EOC and reduced the risk of carbon mineralization. In addition, biochar can increase root biomass and improve root structure, which increase the root exudates, thereby increasing EOC contents (Abiven et al., 2015). However, in CA treatments, high amounts and relatively concentrated biochar application can absorb more water and nutrients from the 0–20 cm soil layer (Zhao et al., 2017). This process was not conducive to the decomposition of organic matter by microorganisms and the production of EOC. Thus, high amounts of biochar application in HA can promote the production of EOC in 0.25–2 mm aggregate, while CA inhibit EOC production. This meant its impact may be limited to the labile OC in specific aggregates after several years of biochar application.

It should be noted that the present study employed only one type of biochar produced from maize straw at a pyrolysis temperature of 450 °C. Indeed, the physicochemical properties of biochar (e.g., porosity, specific surface area, aromaticity, and elemental composition) are largely

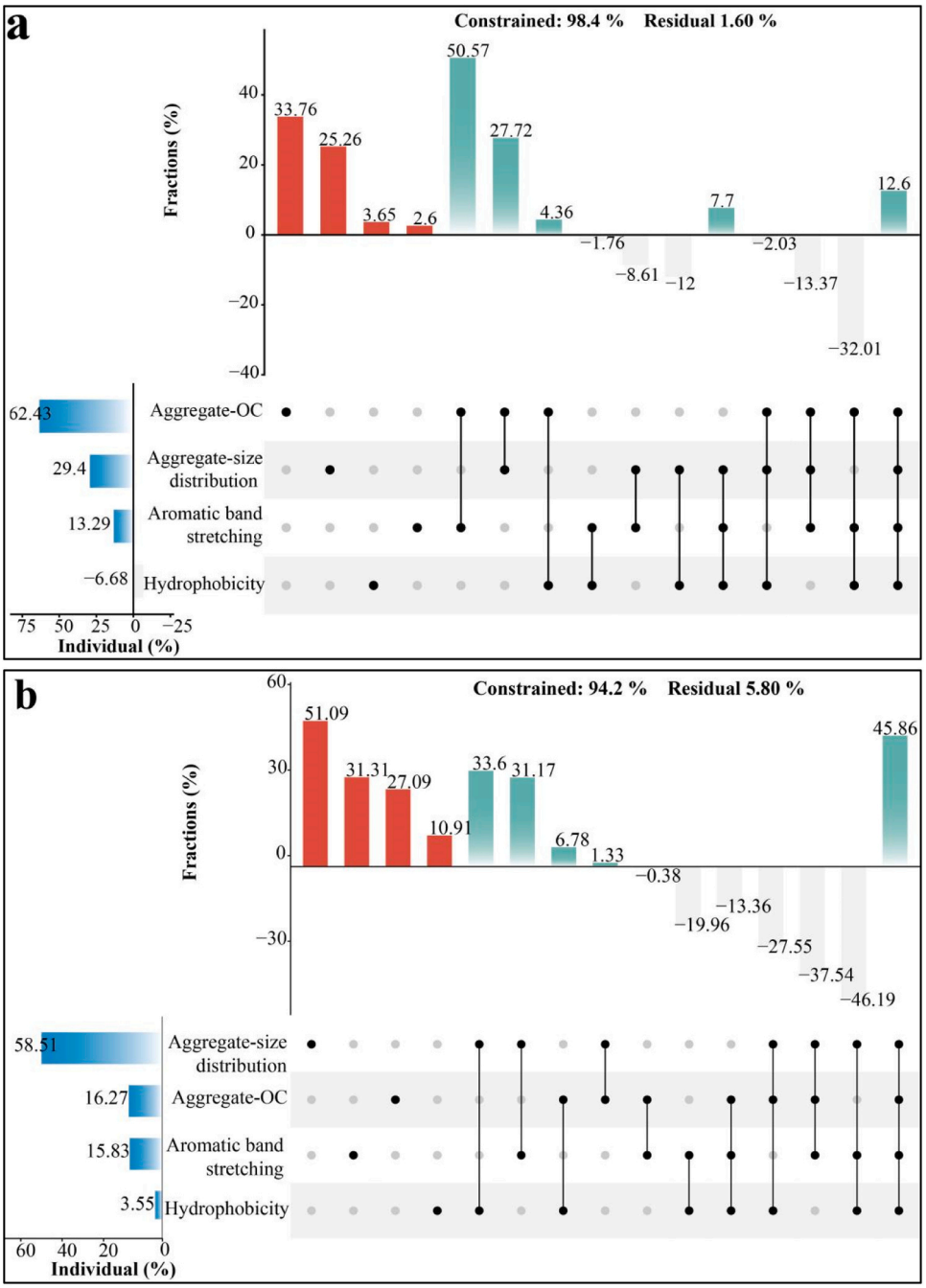

Fig. 6. Variation decomposition and hierarchical segmentation analysis between soil aggregate properties and carbon preservation capacity of total water-stable aggregates in homogeneous application (sub-figure a) and bottom-concentrated application (sub-figure b). In the dot-matrix plot on the right, for each column, the isolated black dot represents the unique effect of each aggregate properties, lines connecting multiple dots represent the common effect of soil aggregate properties. The left blue gradient bars represent the individual effects of soil aggregate properties (hierarchical segmentation analysis). The above red bars and green gradient bars represent the unique and common effect of soil aggregate properties, respectively (variation decomposition analysis).

affected by the type of raw material and pyrolysis conditions, thereby significantly affecting its regulatory effect on soil aggregate distribution and carbon sequestration (Ghorbani and Amirahmadi, 2024; Islam et al., 2021). A recent meta-analysis showed that the high-temperature-produced biochar (>500℃) has a lower atomic ratio of O/C and exhibits strong hydrophobicity (Ghorbani et al., 2023), which considerably lessens the dispersion of soil aggregates and promotes the formation of macroaggregate (Ma et al., 2024), thereby contributing more effectively to long-term carbon stability and aggregate protection. In contrast, biochar generated at lower pyrolysis temperatures (<450℃) contains more volatile components, which can lead to aggregate dispersion and favor the formation of microaggregates (Ghorbani and Amirahmadi, 2024). In addition, wood and straw-derived biochars may have a greater potential for forming soil aggregates since they include a higher percentage of decomposition-resistant components (e.g., lignin and cellulose) that enhance the soil aggregates stability (Ghorbani et al., 2024). Meanwhile, wood and straw-derived biochars have a large specific surface area and high porosity, improving their capacity to absorb and retain soil organic matter in the soil (Asadi et al., 2021). It can be seen that differences in biochar raw materials and pyrolysis conditions lead to significant differences in their properties and functions, thereby affecting their regulatory effects under

different application methods (HA and CA). Therefore, the results of this study have certain limitations. In future research, the characteristics of different types of biochar under different application methods should be further investigated to more deeply clarify their mechanisms of influence on soil structure and carbon stabilization.

4.2. Chemical component of aggregate-organic carbon

Aliphatic-C and aromatic-C had higher resistance to decomposition, and the higher the content, the more stable the SOC (Zhang et al., 2023). We found that HA tended to decrease the hydrophobicity of < 0.25 mm aggregate-OC, while CA increased it (Table 2). This difference may be related to the effect of application method on the distribution of hydrophilic and hydrophobic units. The low soil moisture in the sampling layer in CA reduced the formation of hydrogen bonds between the functional groups of OC and water molecules, thereby decreasing the hydrophilicity of OC (Enaime et al., 2020). The biochar in HA had a larger contact area with the soil, and its surface contained various hydrophilic groups that easily formed hydrogen bonds with water molecules, resulting in increased hydrophilic C═O stretching (Enaime et al., 2020). The hydrophobicity of SOC is obtained by the ratio of hydrophobic groups to hydrophilic groups. Previous studies have shown biochar application can increase the hydrophobicity of bulk soil and aggregate-OC, thereby enhancing soil aggregate stability (Zhang et al., 2019; Situ et al., 2022). Thus, CA may reduce dissociation of < 0.25 mm aggregates by increasing the hydrophobicity of aggregate-OC, thereby enhancing the decomposition resistance of OC. In addition, Zhang et al. (2019) also found that the biochar application caused the organic molecular structure of small macroaggregates to become more hydrophobic and aromatic in a five-year field experiment. Consistently, in this study, 20B and 40B enhanced the aromatic band stretching of < 0.25 mm aggregate-OC in HA (Table 2). This may be due to the biochar contained many highly stable and decomposition-resistant aromatic-C compounds, which selectively accumulated in < 0.25 aggregates after application to the soil, resulting in the enhancement of the aromatic band stretching of < 0.25 aggregate-OC (Deng et al., 2021). Thus, a higher amount of biochar application in HA would change the molecular structure of < 0.25 mm aggregate-OC from simple to complex, making the organic matter difficult to be metabolized and decomposed by soil microorganisms. Overall, the effect of biochar application method and amount on carbon chemical components should be considered in the study of soil carbon sequestration, especially the biochar application method should be emphasized.

4.3. Effect of biochar on soil organic carbon and easily-oxidizable organic carbon

SOC participated in soil microbial activities and nutrient cycling, and was closely related to soil physicochemical properties and crop yield (Bronick and Lal, 2005). Similar to previous reports (Mou et al., 2023), our study also found that all application amounts still increased SOC compared with CK, especially 20B and 40B after six years of one-time application of biochar ($P < 0.05$) (Fig. 1b). This can be attributed to (i) the OC from biochar provided the direct source to the SOC pool (Xu et al., 2024); or (ii) biochar had a large specific surface area and strong adsorption capacity, forming biochar-mineral that was difficult to be decomposed by soil microorganisms (Han et al., 2020); or (iii) biochar increased SOC by increasing aggregate-OC (Fig. S2a, b); or (iv) biochar indirectly increased SOC by promoting root growth and root exudates (Xu et al., 2024). These root-induced processes may further enhance the stabilization of SOC through interactions with minerals and microbial residues (Pausch and Kuzyakov, 201s8); or (v) biochar application increased SOC by affecting the aromatic bands stretching and hydrophobicity of aggregate-OC (Fig. 5c, e). However, CA increased SOC possibly because root growth directly reached or passed through the biochar layer, stimulating the roots to secrete more exudates (Liao et al., 2024), thereby increasing soil dissolved organic carbon (DOC) in the surrounding soil (Fig. S4). Root exudates typically contain organic compounds, some of which may contribute to increasing the DOC pool (Liao et al., 2024). Meanwhile, evaporation-driven capillary rise can transport moisture and dissolved organic compounds upward to the surface under certain conditions (Boduroglu and Bashir, 2022). This mechanism may promote DOC movement to the surface soil (Fig. S4), thereby increasing the accumulation of SOC. In addition, aggregate-OC exhibited significant positive correlations with SOC in CA, suggesting that aggregate-OC was also a crucial factor influencing SOC (Fig. S2b, d). Thus, the effect of HA on SOC was not only related to its properties, but also closely related to its influence on the chemical components of aggregate-OC and crop feedback. The effects of CA on SOC may be driven by root-induced processes, such as increased root exudates and redistribution of DOC through capillary rise.

In addition, our study found that soil EOC decreased after biochar application, but mostly non-significantly (Fig. 1c), which was slightly different from previous studies, reported that biochar application significantly increased soil EOC (Mou et al., 2023; Cheng et al., 2024). This may be because most of the biochar was stored in the soil aggregates as highly stable carbon after six years of biochar application. Meanwhile, the long-term existence of biochar may change the composition of microbial carbon community and affect the decomposition rate of OC, and ultimately reduce the soil EOC (Gross et al., 2021; Kuzyakov et al., 2014). The negative correlation between aggregate-OC and soil EOC also verified this result (Fig. S2a, b). Thus, biochar application did not always increase soil EOC, and application time was key to the effectiveness of biochar application. Overall, biochar improved SOC sequestration in moderately degraded Mollisols by enhancing the stabilization of OC in soil aggregates and root-derived carbon inputs, especially with higher application rates. In contrast, its long-term effect on EOC was limited or even negative, indicating a shift from labile to stable carbon pools that warrants further investigation.

5. Conclusions

After six years of biochar application, higher application amounts still increased SOC and CPC of total water-stable aggregates under the same application methods. Low amount of bottom-concentrated application and high amount of homogeneous application increase aggregate-OC and aggregate-EOC. Bottom-concentrated application increased the hydrophobicity of < 0.25 mm aggregate-OC, while homogeneous application enhanced aromatic band stretching, thereby improving the decomposition resistance of SOC. Homogeneous application may increase SOC by affecting aggregate-OC and its chemical components, while bottom-concentrated application increase it by affecting DOC and aggregate-OC. Overall, to improve SOC sequestration in moderately degraded Mollisols, a low amount of bottom-concentrated application (10 Mg ha^{-1}) and a higher amount of homogeneous application (≥20 Mg ha^{-1}) should be considered under crop planting. These insights provide a mechanistic basis for optimizing biochar application methods and amounts to maximize long-term organic carbon sequestration and improve soil structure in intensive cropping systems.

CRediT authorship contribution statement

Pengke Yan: Visualization, Investigation, Conceptualization. **Zhimiao Wei:** Investigation. **Xiaoguang Niu:** Visualization, Investigation. **Haijun Zhang:** Visualization, Investigation. **Sihua Yan:** Writing – original draft, Visualization, Investigation, Formal analysis, Data curation, Conceptualization. **Shaoliang Zhang:** Writing – review & editing, Supervision, Methodology, Funding acquisition, Conceptualization.

Declaration of Competing Interest

The authors declare that they have no known competing financial

interests or personal relationships that could have appeared to influence the work reported in this paper.

Acknowledgments

Thanks to Muhammad Aurangzeib, who helped us in editing language. This work was sponsored by the Natural Science Foundation of Heilongjiang Province (Key project) (ZL2024D001) and the National Natural Science Foundation of China (42177321).

Appendix A. Supporting information

Supplementary data associated with this article can be found in the online version at doi:10.1016/j.still.2025.106795.

Data availability

The data that has been used is confidential.

References

Abiven, S., Hund, A., Martinsen, V., Cornelissen, G., 2015. Biochar amendment increases maize root surface areas and branching: a shovelomics study in Zambia. Plant Soil 395, 45–55. https://doi.org/10.1007/s11104-015-2533-2.

Asadi, H., Ghorbani, M., Rezaei-Rashti, M., Abrishamkesh, S., Amirahmadi, E., Chen, C., Gorji, M., 2021. Application of rice husk biochar for achieving sustainable agriculture and environment. Rice Sci. 28, 325–343. https://doi.org/10.1016/j.rsci.2021.05.004.

Blair, G.J., Lefroy, R.D., Lisle, L., 1995. Soil carbon fractions based on their degree of oxidation, and the development of a carbon management index for agricultural systems. Aust. J. Agric. Res. 46, 1459–1466. https://doi.org/10.1071/AR9951459.

Boduroglu, S., Bashir, R., 2022. Review of capillary rise experiments for surface-active solutes in the subsurface. Geotechnics 2, 706–730. https://doi.org/10.3390/geotechnics2030034.

Bronick, C.J., Lal, R., 2005. Soil structure and management: a review. Geoderma 124, 3–22. https://doi.org/10.1016/j.geoderma.2004.03.005.

Capriel, P., 1997. Hydrophobicity of organic matter in arable soils: influence of management. Eur. J. Soil Sci. 48, 457–462. https://doi.org/10.1111/j.1365-2389.1997.tb00211.x.

Chen, J., Zhou, J., Zheng, W., Leng, S., Ai, Z., Zhang, W., Yang, Z., Yang, J., Xu, Z., Cao, J., 2024b. A complete review on the oxygen-containing functional groups of biochar: formation mechanisms, detection methods, engineering, and applications. Sci. Total Environ. 946, 174081. https://doi.org/10.1016/j.scitotenv.2024.174081.

Chen, Y., Sun, K., Yang, Y., Gao, B., Zheng, H., 2024a. Effects of biochar on the accumulation of necromass-derived carbon, the physical protection and microbial mineralization of soil organic carbon. Crit. Rev. Environ. Sci. Technol. 54, 39–67. https://doi.org/10.1080/10643389.2023.2221155.

Chen, Z., Jin, P., Wang, H., Hu, T., Lin, X., Xie, Z., 2022. Ecoenzymatic stoichiometry reveals stronger microbial carbon and nitrogen limitation in biochar amendment soils: a meta-analysis. Sci. Total Environ. 838. https://doi.org/10.1016/j.scitotenv.2022.156532.

Cheng, Z., Guo, J., Jin, W., Liu, Z., Wang, Q., Zha, L., Zhou, Z., Meng, Y., 2024. Responses of SOC, labile SOC fractions, and amino sugars to different organic amendments in a coastal saline-alkali soil. Soil Tillage Res. 239. https://doi.org/10.1016/j.still.2024.106051.

Cui, B., Cui, E., Hu, C., Fan, X., Gao, F., 2020. Effects of selected biochars application on the microbial community structures and diversities in the rhizosphere of water spinach (*ipomoea aquatica* Forssk.) irrigated with reclaimed water. Environ. Sci. 41, 5636–5647.

Dal Ferro, N., Stevenson, B., Morari, F., Müller, K., 2023. Long-term tillage and irrigation effects on aggregation and soil organic carbon stabilization mechanisms. Geoderma 432, 116398. https://doi.org/10.1016/j.geoderma.2023.116398.

Deiss, L., Sall, A., Demyan, M.S., Culman, S.W., 2021. Does crop rotation affect soil organic matter stratification in tillage systems? Soil Tillage Res. 209. https://doi.org/10.1016/j.still.2021.104932.

Deng, H., Gao, M., Long, Y., Lai, J.X., Wang, Y.Y., Wang, Z.F., 2021. Effects of biochar and straw return on soil aggregate and organic carbon on purple soil dry slope land. Environ. Sci. 42, 5481–5490.

Ellerbrock, R.H., Gerke, H.H., Bachmann, J., Goebel, M.O., 2005. Composition of organic matter fractions for explaining wettability of three forest soils. Soil Sci. Soc. Am. J. 69, 57–66. https://doi.org/10.2136/sssaj2005.0057.

Enaime, G., Bacaoui, A., Yaacoubi, A., Luebken, M., 2020. Biochar for wastewater treatment-conversion technologies and applications. Appl. Sci. Basel 10. https://doi.org/10.3390/app10103492.

Francoys, A., Li, H., Mendoza, O., Dewitte, K., Bode, S., Boeckx, P., Cornelis, W., De Neve, S., Sleutel, S., 2024. Control of landscape position on organic matter decomposition via soil moisture during a wet summer. Soil Tillage Res. 244. https://doi.org/10.1016/j.still.2024.106277.

Gao, L., Wang, J., Li, S., Wu, H., Wu, X., Liang, G., Gong, D., Zhang, X., Cai, D., Degre, A., 2019b. Soil wet aggregate distribution and pore size distribution under different tillage systems after 16 years in the loess plateau of China. Catena 173, 38–47. https://doi.org/10.1016/j.catena.2018.09.043.

Gao, L., Wang, B., Li, S., Han, Y., Zhang, X., Gong, D., Ma, M., Liang, G., Wu, H., Wu, X., Cai, D., Degre, A., 2019a. Effects of different long-term tillage systems on the composition of organic matter by ^{13}C CP/TOSS NMR in physical fractions in the loess plateau of China. Soil Tillage Res. 194. https://doi.org/10.1016/j.still.2019.104321.

Ghorbani, M., Amirahmadi, E., 2024. Insights into soil and biochar variations and their contribution to soil aggregate status - a meta-analysis. Soil Tillage Res. 244, 106282. https://doi.org/10.1016/j.still.2024.106282.

Ghorbani, M., Neugschwandtner, R.W., Soja, G., Konvalina, P., Kopecky, M., 2023. Carbon fixation and soil aggregation affected by biochar oxidized with hydrogen peroxide: considering the efficiency of pyrolysis temperature. Sustainability 15, 7158. https://doi.org/10.3390/su15097158.

Ghorbani, M., Konvalina, P., Neugschwandtner, R.W., Soja, G., Barta, J., Chen, W.H., Amirahmadi, E., 2024. How do different feedstocks and pyrolysis conditions effectively change biochar modification scenarios? A critical analysis of engineered biochars under H_2O_2 oxidation. Energy Convers. Manag. Energy Convers. Manag. 300, 117924. https://doi.org/10.1016/j.enconman.2023.117924.

Gross, A., Bromm, T., Glaser, B., 2021. Soil organic carbon sequestration after biochar application: a global meta-analysis. Agron. Basel 11. https://doi.org/10.3390/agronomy11122474.

Han, L., Sun, K., Yang, Y., Xia, X., Li, F., Yang, Z., Xing, B., 2020. Biochar's stability and effect on the content, composition and turnover of soil organic carbon. Geoderma 364. https://doi.org/10.1016/j.geoderma.2020.114184.

Heikkinen, J., Keskinen, R., Soinne, H., Hyvaluoma, J., Nikama, J., Wikberg, H., Kalli, A., Siipola, V., Melkior, T., Dupont, C., Campargue, M., Larsson, S.H., Hannula, M., Rasa, K., 2019. Possibilities to improve soil aggregate stability using biochars derived from various biomasses through slow pyrolysis, hydrothermal carbonization, or torrefaction. Geoderma 344, 40–49. https://doi.org/10.1016/j.geoderma.2019.02.028.

Huang, R., Gao, X., Wang, F., Xu, G., Long, Y., Wang, C., Wang, Z., Gao, M., 2020. Effects of biochar incorporation and fertilizations on nitrogen and phosphorus losses through surface and subsurface flows in a sloping farmland of entisol. Agric. Ecosyst. Environ. 300. https://doi.org/10.1016/j.agee.2020.106988.

Islam, M.U., Jiang, F., Guo, Z., Peng, X., 2021. Does biochar application improve soil aggregation? A meta-analysis. Soil Tillage Res. 209, 104926. https://doi.org/10.1016/j.still.2020.104926.

Jia, H., Zhao, Y., Deng, H., Yu, H., Feng, D., Zhang, Y., Ge, C., Li, J., 2023. Significant contributions of biochar-derived dissolved matters to ecotoxicity to earthworms (*eisenia fetida*) in soil with biochar amendment. Environ. Technol. Innov. 29, 102988. https://doi.org/10.1016/j.eti.2022.102988.

Kalembasa, S.J., Jenkinson, D.S., 1973. A comparative study of titrimetric and gravimetric methods for the determination of organic carbon in soil. J. Sci. Food Agric. 24, 1085–1090. https://doi.org/10.1002/jsfa.2740240910.

Kan, Z., Ma, S., Liu, Q., Liu, B., Virk, A., Qi, J., Zhao, X., Lal, R., Zhang, H., 2020. Carbon sequestration and mineralization in soil aggregates under long-term conservation tillage in the north China plain. Catena 188. https://doi.org/10.1016/j.catena.2019.104428.

Kuzyakov, Y., Bogomolova, I., Glaser, B., 2014. Biochar stability in soil: decomposition during eight years and transformation as assessed by compound-specific ^{14}C analysis. Soil Biol. Biochem. 70, 229–236. https://doi.org/10.1016/j.soilbio.2013.12.021.

Lai, J., Zou, Y., Zhang, J., Peres-Neto, P.R., 2022. Generalizing hierarchical and variation partitioning in multiple regression and canonical analyses using the rdacca. Hp r package. Methods Ecol. Evol. 13, 782–788. https://doi.org/10.1111/2041-210X.13800.

Laudicina, V.A., Novara, A., Barbera, V., Egli, M., Badalucco, L., 2015. Long-term tillage and cropping system effects on chemical and biochemical characteristics of soil organic matter in a Mediterranean semiarid environment. Land Degrad. Dev. 26, 45–53. https://doi.org/10.1002/ldr.2293.

Li, S., Lu, J., Liang, G., Wu, X., Zhang, M., Plougonven, E., Wang, Y., Gao, L., Abdelrhman, A.A., Song, X., Liu, X., Degre, A., 2021a. Factors governing soil water repellency under tillage management: the role of pore structure and hydrophobic substances. Land Degrad. Dev. 32, 1046–1059. https://doi.org/10.1002/ldr.3779.

Li, S., Cui, Y., Moorhead, D.L., Dijkstra, F.A., Sun, L., Xia, Z., Gao, Y., Ma, Q., Yu, W., 2025. Phosphorus limitation regulates the responses of microbial carbon metabolism to long-term combined additions of nitrogen and phosphorus in a cropland. Soil Biol. Biochem. 200. https://doi.org/10.1016/j.soilbio.2024.109614.

Li, W., Duan, F., Zhao, Q., Song, W., Cheng, Y., Wang, X., Li, L., He, K., 2021b. Investigating the effect of sources and meteorological conditions on wintertime haze formation in northeast China: a case study in harbin. Sci. Total Environ. 801. https://doi.org/10.1016/j.scitotenv.2021.149631.

Li, Y., Li, Z., Cui, S., Liang, G., Zhang, Q., 2021c. Microbial-derived carbon components are critical for enhancing soil organic carbon in no-tillage croplands: a global perspective. Soil Tillage Res. 205. https://doi.org/10.1016/j.still.2020.104758.

Liao, L., Wang, J., Dijkstra, F.A., Lei, S., Zhang, L., Wang, X., Liu, G., Zhang, C., 2024. Nitrogen enrichment stimulates rhizosphere multi-element cycling genes via mediating plant biomass and root exudates. Soil Biol. Biochem. 190. https://doi.org/10.1016/j.soilbio.2023.109306.

Liu, X., Zhang, S., Zhang, X., Ding, G., Cruse, R.M., 2011. Soil erosion control practices in northeast China: a mini-review. Soil Tillage Res. 117, 44–48. https://doi.org/10.1016/j.still.2011.08.005.

Ma, S., Cao, Y., Lu, J., Ren, T., Cong, R., Lu, Z., Zhu, J., Li, X., 2024. Response of soil aggregation and associated organic carbon to organic amendment and its controls: a global meta-analysis. CATENA 237, 107774. https://doi.org/10.1016/j.catena.2023.107774.

Mou, Z.Y., Shen, Y.Y., Cao, Y., Wang, Z.H., Chen, Y.S., Teng, Q.M., Huang, K.C., Mao, X. Y., Xu, G.P., 2023. Effects of biochar application on soil organic carbon component in *eucalyptus* plantations after five years in Northern guangxi. Environ. Sci. 44, 6869–6879.

Ndzelu, B.S., Dou, S., Zhang, X., Zhang, Y., Ma, R., Liu, X., 2021. Tillage effects on humus composition and humic acid structural characteristics in soil aggregate-size fractions. Soil Tillage Res. 213. https://doi.org/10.1016/j.still.2021.105090.

Peltre, C., Gregorich, E.G., Bruun, S., Jensen, L.S., Magid, J., 2017. Repeated application of organic waste affects soil organic matter composition: evidence from thermal analysis, FTIR-PAS, amino sugars and lignin biomarkers. Soil Biol. Biochem. 104, 117–127. https://doi.org/10.1016/j.soilbio.2016.10.016.

Reddy, K.R., Xie, T., Dastgheibi, S., 2014. Evaluation of biochar as a potential filter media for the removal of mixed contaminants from urban storm water runoff. J. Environ. Eng. 140. https://doi.org/10.1061/(ASCE)EE.1943-7870.0000872.

Sanchez, G., 2013. PLS path modeling with r. Berkeley. Trowchez Ed. 383, 551.

Schmitz, O.J., Sylven, M., Atwood, T.B., Bakker, E.S., Berzaghi, F., Brodie, J.F., Cromsigt, J.P.G.M., Tilker, A.B., Leroux, S.J., Schepers, F.J., Smith, F.A., Stark, S., Svenning, J.-C., Tilker, A.B., Ylanne, H., 2023. Trophic rewilding can expand natural climate solutions. Nat. Clim. Change 13, 324–333. https://doi.org/10.1038/s41558-023-01631-6.

Shen, W.S., Cao, X.Z., Shen, F.Y., 2006. Classification and grading of land degradation in China. J. Ecol. Rural Environ. 22, 88–93.

Simon, T., Javurek, M., Mikanova, O., Vach, M., 2009. The influence of tillage systems on soil organic matter and soil hydrophobicity. Soil Tillage Res. 105, 44–48. https://doi.org/10.1016/j.still.2009.05.004.

Singh, P., Benbi, D.K., 2018. Soil organic carbon pool changes in relation to slope position and land-use in Indian lower Himalayas. Catena 166, 171–180. https://doi.org/10.1016/j.catena.2018.04.006.

Situ, G., Zhao, Y., Zhang, L., Yang, X., Chen, D., Li, S., Wu, Q., Xu, Q., Chen, J., Qin, H., 2022. Linking the chemical nature of soil organic carbon and biological binding agent in aggregates to soil aggregate stability following biochar amendment in a rice paddy. Sci. Total Environ. 847. https://doi.org/10.1016/j.scitotenv.2022.157460.

Six, J., Elliott, E., Paustian, K., Doran, J., 1998. Aggregation and soil organic matter accumulation in cultivated and native grassland soils. Soil Sci. Soc. Am. J. 62, 1367–1377. https://doi.org/10.2136/sssaj1998.03615995006200050032x.

Sun, Q., Yang, X., Bao, Z., Gao, J., Meng, J., Han, X., Lan, Y., Liu, Z., Chen, W., 2022. Responses of microbial necromass carbon and microbial community structure to straw- and straw-derived biochar in brown earth soil of northeast China. Front. Microbiol. 13. https://doi.org/10.3389/fmicb.2022.967746.

Tivet, F., de Moraes Sa, J.C., Lal, R., Bastos Pereira Milori, D.M., Briedis, C., Letourmy, P., Pinheiro, L.A., Borszowskei, P.R., Hartman, Dd.C., 2013. Assessing humification and organic c compounds by laser-induced fluorescence and FTIR spectroscopies under conventional and no-till management in Brazilian oxisols. Geoderma 207, 71–81. https://doi.org/10.1016/j.geoderma.2013.05.001.

Visiy, E.B., Djousse, B.M.K., Martin, L., Zangue, C.N., Sangodoyin, A., Gbadegesin, A.S., Fonkou, T., 2022. Effectiveness of biochar filters vegetated with *echinochloa pyramidalis* in domestic wastewater treatment. Water Sci. Technol. 85, 2613–2624. https://doi.org/10.2166/wst.2022.147.

Wang, H., Yang, S., Wang, Y., Gu, Z., Xiong, S., Huang, X., Sun, M., Zhang, S., Guo, L., Cui, J., 2022. Rates and causes of black soil erosion in northeast China. Catena 214, 106250. https://doi.org/10.1016/j.catena.2022.106250.

Xiao, Y., Zhou, M., Li, Y., Zhang, X., Wang, G., Jin, J., Ding, G., Zeng, X., Liu, X., 2022. Crop residue return rather than organic manure increases soil aggregate stability under corn-soybean rotation in surface mollisols. Agric. Basel 12. https://doi.org/10.3390/agriculture12020265.

Xing, Z., Tian, K., Du, C., Li, C., Zhou, J., Chen, Z., 2019. Agricultural soil characterization by FTIR spectroscopy at micrometer scales: depth profiling by photoacoustic spectroscopy. Geoderma 335, 94–103. https://doi.org/10.1016/j.geoderma.2018.08.003.

Xu, P., Zhu, J., Wang, H., Shi, L., Zhuang, Y., Fu, Q., Chen, J., Hu, H., Huang, Q., 2021. Regulation of soil aggregate size under different fertilizations on dissolved organic matter, cellobiose hydrolyzing microbial community and their roles in organic matter mineralization. Sci. Total Environ. 755. https://doi.org/10.1016/j.scitotenv.2020.142595.

Xu, P., Wang, Q., Duan, C., Huang, G., Dong, K., Wang, C., 2024. Biochar addition promotes soil organic carbon sequestration dominantly contributed by macro-aggregates in agricultural ecosystems of China. J. Environ. Manag. 359, 121042. https://doi.org/10.1016/j.jenvman.2024.121042.

Yan, S., Zhang, S., Yan, P., Aurangzeib, M., 2022. Effect of biochar application method and amount on the soil quality and maize yield in mollisols of northeast China. Biochar 4 (1). https://doi.org/10.1007/s42773-022-00180-z.

Yan, S., Zhang, S., Yan, P., Wei, Z., Wang, H., Zhang, H., Niu, X., Aurangzeib, M., Tao, G., 2025. Biochar application strategies mediating the soil temperature, moisture and salinity during the crop seedling stage in mollisols. Sci. Total Environ. 958, 178098. https://doi.org/10.1016/j.scitotenv.2024.178098.

Yang, Y., Wu, J., Zhao, S., Gao, C., Pan, X., Tang, D.W.S., van der Ploeg, M., 2021. Effects of long-term super absorbent polymer and organic manure on soil structure and organic carbon distribution in different soil layers. Soil Tillage Res. 206. https://doi.org/10.1016/j.still.2020.104781.

Yang, Y., Sun, K., Han, L., Chen, Y., Liu, J., Xing, B., 2022. Biochar stability and impact on soil organic carbon mineralization depend on biochar processing, aging and soil clay content. Soil Biol. Biochem. 169. https://doi.org/10.1016/j.soilbio.2022.108657.

Zhang, F., Qiao, Y., Miao, S., Han, X., 2016. Chemical structure characteristics of all fractionations in mollisol organic matter under long-term continuous maize cropping. Sci. Agric. Sin. 49, 1913–1924.

Zhang, J., Wei, Y., Liu, J., Yuan, J., Liang, Y., Ren, J., Cai, H., 2019. Effects of maize straw and its biochar application on organic and humic carbon in water-stable aggregates of a mollisol in northeast China: a five-year field experiment. Soil Tillage Res. 190, 1–9. https://doi.org/10.1016/j.still.2019.02.014.

Zhang, Q., Du, Z., Lou, Y., He, X., 2015. A one-year short-term biochar application improved carbon accumulation in large macroaggregate fractions. Catena 127, 26–31. https://doi.org/10.1016/j.catena.2014.12.009.

Zhang, X., Shen, S., Xue, S., Hu, Y., Wang, X., 2023. Long-term tillage and cropping systems affect soil organic carbon components and mineralization in aggregates in semiarid regions. Soil Tillage Res. 231. https://doi.org/10.1016/j.still.2023.105742.

Zhao, L., Chen, J., Li, H., Liang, N., Zhang, P., 2017. Effect of pyrolysis temperature and acid treatment on the generation of free radicals in biochars. Environ. Chem. 36, 2472–2478.

Zhou, H., Fang, H., Zhang, Q., Wang, Q., Chen, C., Mooney, S.J., Peng, X., Du, Z., 2019. Biochar enhances soil hydraulic function but not soil aggregation in a sandy loam. Eur. J. Soil Sci. 70 (2), 291–300. https://doi.org/10.1111/ejss.12732.

Zhu, L., Zhang, F., Li, L., Liu, T., 2021. Soil c and aggregate stability were promoted by bio-fertilizer on the north China plain. J. Soil Sci. Plant Nutr. 21, 2355–2363. https://doi.org/10.1007/s42729-021-00527-8.